DYNAMIC MODELING AND EXPERIMENTAL VALIDATION OF AN ELECTRICAL WATER HEATER WITH A DOUBLE STORAGE TANK CONFIGURATION

Nicolas Leclercq[1]*, Simon Marichal[1], Sylvain Quoilin[1], Vincent Lemort[1]

[1] Thermodynamics Laboratory, University of Liège, 4000 Liège, Belgium

*Correspoding Author: N.Leclercq@ULiege.be

ABSTRACT

This paper presents a study of an electrical water-heater using two storage tanks connected in series. This particular configuration is intended to reduce the thickness of the wall-mounted water heater by using two small-diameter cylindrical tanks instead of a single large-diameter tank.
To conduct this study, a Python dynamic model of the water heater has been developed, requiring 3 empirical parameters. The model uses a multi-node modeling approach to account for the temperature stratification inside the two storage tanks, as it provided a good accuracy with a low computation time. Moreover, an optimization technique allowing to reduce the computation time is proposed. When using 40 layers in each storage tank, the model is able to simulate real conditions 35000 times faster than real time. Therefore, the model is well-suited for model-based control design and will, in the future, be used to model a fleet of water heaters providing ancillary services to the transmission system operator in the Belgian grid.
Ultimately, the paper describes an experimental study conducted to validate the dynamic model. In this experimental work, the water heater's electricity consumption is assessed across a daily water usage scenario. The measurements also allow to capture the ambient heat losses and the temperature stratification profiles inside the tanks.

1 INTRODUCTION

The energy transition aims to reduce the carbon footprint associated with energy production, leading to a decrease in the carbon dioxide (CO_2) footprint of electricity generation. In Belgium, the part of electricity produced by variable energy sources is growing, from 2% in 2008 to 20% in 2022 (IEA) as can shown in **Figure** 1. Nevertheless, this increasing penetration of renewable energy sources such as wind or solar requires additional balancing services in the transmission and in the distribution grids.
The interest of Electric Water Heaters (EWH) as decentralized flexibility resources to provide such services is two-fold:

- They only use electricity as an energy source, making them a suitable technology to decrease the carbon footprint of the residential sector. Furthermore, using heat-pump water heaters increases the performance of such technology and decreases its carbon footprint, provided that the refrigerant has a low global warming potential.
- They can be used as energy storage device when shifting the heating of water or heating the water at higher temperatures to absorb the excess of electricity production. They can therefore be used, with dedicated control strategies, in enhancing demand response to balance the network. Diao et al. (2012) investigated different control strategies for demand response and network frequency regulation by overheating the water inside a pool of 147 EWHs. They have shown that EWH's

https://doi.org/10.52202/077185-0015

can be controlled using centralized signal and that a step change in the temperature setting is effective with little time delay. Quynh et al. (2022) have built an aggregated model to estimate the power consumption of a pool of 6000 EWH's and have found a relation between the average tank bottom temperature of the pool and the total power consumption.

The accurate modeling of a single electrical water heater is essential to estimate the power consumption of a pool of electrical water heaters and its potential to enhance demand response. The modeling of such a system relies on the prediction of the temperature stratification profile occurring inside the storage tank, created by the density difference between warm fluid and cold fluid. This stratification can be difficult to model and is still an active research field. The degree of stratification of a tank and the way of modeling it depends on its design: size, location, design of inlets and outlets ports and mass flow rates entering/leaving the tank (Duffie and Beckman, 2013).

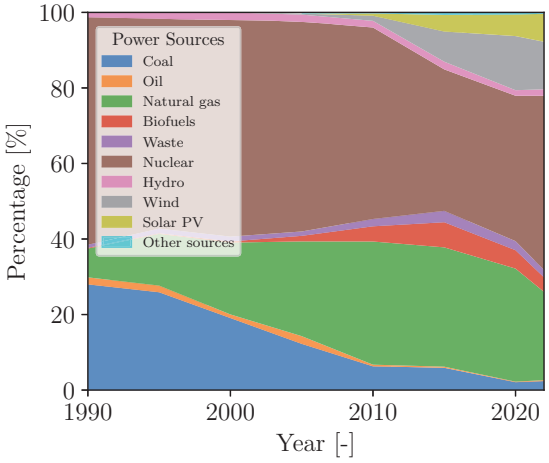

Figure 1: Evolution over time in the electricity generation sources of Belgium (IEA).

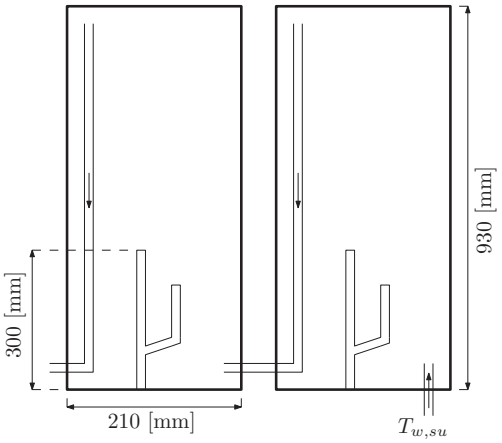

Figure 2: Dimensions of the Velis water heater.

The paper presents a study of an EWH with a specific geometry: it is composed by two tanks placed in series to increase the stratification effect (increases the total height). It provides a validated model of the studied EWH allowing to predict its performance 35000 times faster than its real-time behavior. Details of the model are given as well as the control strategy implemented to mimic its behavior and predict the power consumption and water outlet temperature varying with time.

2 DYNAMIC MODELING OF THE WATER HEATER

The objective of the dynamic modeling of the EWH is to reproduce the power response (power consumption) and outlet temperature as a function of the time, considering a large time-scale (several weeks can be simulated). The main input of the model is the water consumption over time and, along with a control strategy and a temperature set point (T_{SP}), it enables the identification of the heating system operating conditions. As shown in **Figure** 3, the model requires as parameter the EWH geometry, three empirical coefficients and the initial and external temperature boundary conditions.

The modeling of a water heater can be split into two parts: the modeling of the storage tank (to take into account temperature stratification) and the modeling of the heating technology (heat exchangers for heat pumps or electrical resistor). The modeling of the heating technology is simple when using a heating resistor: a constant-power heat generation is added inside the storage, whatever the temperature of the fluid surrounding the resistor. Regarding the storage, the modeling is more challenging, but a lot of different techniques already exist. According to Dumont et al. (2016), 8 kinds of storage tank modeling

https://doi.org/10.52202/077185-0015

approaches are used in the literature. Among them can be found:

- Fully mixed storage (no temperature stratification, 0D model)
- Moving-boundary and plug flow (two main temperature zones, 1D model)
- Multiple-node (division in several zones, 1D or 2D model)
- Computational Fluid Dynamics (CFD, 2D or 3D model)
- Analytical solutions (1D model)

Lots of examples of storage tanks modeling can be found in the literature, for instance, Salameh et al. (2021) used an homogeneous (fully-mixed) model to predict the outlet temperature of a water heater. They however only validated the heating phase and therefore do not need to consider the dynamics of the discharge period. Their model allowed them to perform a geometry optimization and to figure out that a minimum volume with a maximum power allowed the most energy savings. In Missaoui et al. (2023), the authors used a CFD model to accurately predict the temperature stratification in a heat pump water heater using an immersed helical coil heat exchanger, useful to predict the heat exchanger capacity. It is however too computationally heavy to be used for long dynamic simulations. In Powell and Edgar (2013) and Dickes et al. (2015), the authors developed an improved plug-flow model to represent a thermocline storage, where the prediction of the thermocline profile is as accurate as in a multi-node model for most transient and steady-state conditions but 99% faster. It however does not allow to predict temperature stratification if a heating source is placed inside the storage tank. When a heating source is used, analytical and multi-node models seem to be the most efficient. For instance, Xu et al. (2014) compared an analytical model, a plug-in model and a homogeneous model and concluded that the analytical is the only model allowing heating and turn-off action when simulating the dynamic behavior (power response) over 12 hours. Moreover, Beeker et al. (2015), use an analytical water heater model to quantify the potential in demand response program. Their model, though complex, accurately represents the behavior of a 200 L water heater tested experimentally with a 24-hour water-usage scenario simulated in 4.6 seconds. When more simplicity is needed, multiple node model can also be very efficient. Several authors make use of this simplicity, for example Quynh et al. (2022) is used a multi-node model to create an empirical model of aggregated water heaters estimating the power consumption of 6000 water heaters throughout the day. Nevertheless, the model is not validated using experimental data. In Nash et al. (2017), the authors present a very efficient multi-node model to predict the outlet temperature of a HPWH, experimentally validated with several thermoclines in the storage tank. Finally, zonal models can also be used when more precision is needed, as an example, Deutz et al. (2016) developed a 2-dimensional multi-node model (zonal model) used to predict the performance of a heat-pump water heater with high precision in the results. From the examples previously cited and as already predicted by Dumont et al. (2016), when dynamic results are needed, with medium to low computational time and no accuracy in the local phenomena, and using a heat source inside the storage tank, the multiple-node model seems to be an appropriate choice.
The model presented in this paper is a multi-node model. The selection of the time steps and number of nodes is analyzed, moreover, using a computational time optimization methodology allows to reach a real time to computational time ratio of 35000. Moreover, the experimental data acquired to validate the model is thoroughly analyzed and the model is provided under an open license (see conclusion for the GitHub link).

2.1 The Ariston Velis electrical water heater

The studied electrical water heater has a specific geometry: it is composed of two storage tanks placed in series, with heating resistors placed at the bottom of each of them. A diagram of the modeled and tested water heater can be found in **Figure** 2. According to the patent of this specific geometry of EWH (Paolesi and Stopponi, 2011), it allows a thinner geometry for the given volume, it allows to heat only one part of the stored water when this is sufficient for the expected consumption and it allows to get a lower manufacturing cost due to a decreased storage volume V_{sto} for the same usable volume (V_u) of water at a usable temperature (T_u) of a standard storage water heater. Despite this decrease of storage volume, the usable volume is the same for two reasons:

https://doi.org/10.52202/077185-0015

- The mixing effect is lower due to the decreased diameter of the tank where the cold water enters (the closer the diameter of the tank and the inlet pipe, the lower the mixing effect)
- The water storage temperature (T_{sto}) can be increased without increasing heat losses as the shell surface is reduced due to the reduced volume for a same usable volume.

The usable volume is defined as follow:

$$V_u = V_{sto} \frac{(T_{sto} - T_{w,su})}{(T_u - T_{w,su})} \tag{1}$$

where T_u is the temperature used by the user resulting in the mixing of the storage water at temperature T_{sto} and the cold (network) water at temperature $T_{w,su}$.
Heating resistors with 1350 W of nominal power are located at the bottom of each tank, allowing to heat up the tanks independently. The control system makes use of PT100 temperature sensors located just above the heating resistor of each tank in order to know when the tanks need to be heated.

2.2 Multi-node modeling of the storage tank

The multi-node modeling approach used is inspired from the model developed by Nash et al. (2017). A storage tank is divided vertically in n number of layers (or nodes), where the water properties (density, specific heat capacity) are constant and the water temperature uniform. Heat exchanges between adjacent layers occur vertically, while heat exchanges with the environment occur horizontally. A diagram of a layer and its mass and heat exchanges with the adjacent layers and environment can be found in **Figure** 4.

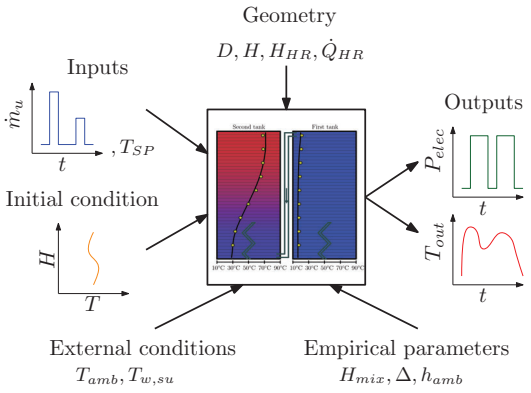

Figure 3: Definition of the inputs, outputs and parameters interacting with the model.

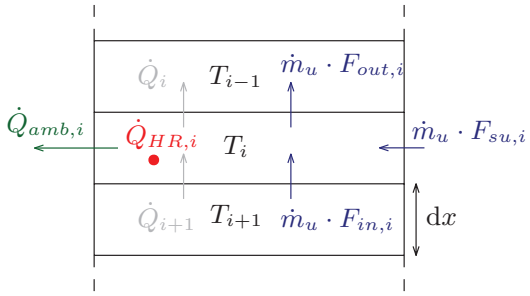

Figure 4: Heat and mass exchange of a layer in the multi-node model.

The height of the layer dx is defined as the height of the storage divided by the number of layers n. In this diagram, $\dot{Q}_i$ represents the rate of heat exchange between the layer i and the layer $i-1$, occurring by conduction but also convection due to a density difference between the layers as will be explained further. $\dot{Q}_{HR,i}$ represents the heat generation rate that can come for instance from a heating resistor while $\dot{Q}_{amb,i}$ embodies the ambient losses. The mass exchange is depicted by the term $\dot{m}_u$ which is simply the usage mass flow rate. This usage flow rate can be injected in several nodes at the same time (usually the bottom nodes) and some functions F_{out}, F_{in} and F_{su} allow to define the distribution of this flow rate into the involved nodes. The empirical parameter H_{mix} allows to define the height at which the supply water is injected from the bottom. The number of layers involved in this distribution can thus be defined as:

$$k_l = H_{mix}/\mathrm{d}x \tag{2}$$

The distribution in the latter k_l nodes is therefore governed by the functions $F_{su,i} = 1/k_l$, $F_{in,i} = (n -$

https://doi.org/10.52202/077185-0015

$i)/k_l$, $F_{out,i} = (n - i + 1)/k_l$ in the following energy conservation equation. Regarding the nodes not directly affected by the supply water injection, the following functions govern the mass balance: $F_{su,i} = 0$, $F_{in,i} = F_{out,i} = 1$.
The conservation of energy is applied in each layer to obtain the temperature profile in the tank. For the i^{th} layer, the equation is written as:

$$m_i c_p \frac{\mathrm{d}T_i}{\mathrm{d}t} = k_{HR}\dot{Q}_{HR,i} + \dot{Q}_{i+1} - \dot{Q}_i + F_{in,i}\dot{m}_u c_p T_{i+1} - F_{out,i}\dot{m}_u c_p T_i + F_{su,i}\dot{m}_u c_p T_{w,su} - \dot{Q}_{amb,i} \quad (3)$$

where k_{HR} is an activation parameter of the heating resistor simulating a switch. When discretized using a time step τ, the first term of the equation can be rewritten using the backward Euler method:

$$m_i c_p \frac{\mathrm{d}T_i}{\mathrm{d}t} = m_i c_p \frac{(T_i^t - T_i^{t-1})}{\tau} \quad (4)$$

where T_i^t is the unknown new temperature of the layer and T_i^{t-1} the temperature at the previous time (known). The heat exchange with the ambient can be developed as:

$$\dot{Q}_{amb,i}^t = h_{amb} A_{amb,i} (T_i^t - T_{amb}) \quad (5)$$

where h_{amb} is an empirical heat transfer coefficient between the water and the surrounding temperature, $A_{amb,i}$ is the surface area of node i exposed to the surrounding, and T_{amb} is the ambient temperature. As shown in **Equation** 5, a constant heat transfer coefficient has been chosen to model the heat exchange between the hot water and the ambient air. This can be justified by the thick insulation layer placed around the tank that has a low heat conductivity, making the global coefficient almost constant even when the convection coefficients of the water or the air vary. Regarding the heat exchange between two layers, it can be written as:

$$\dot{Q}_i^t = K_{i-1} A_c (T_i^t - T_{i-1}^t) \quad (6)$$

where A_c is the horizontal cross-sectional area of the tank and K_{i-1} is a modified conductivity coefficient, taking into account a convection effect when a colder layer is above a hotter layer. This heat transfer coefficient is therefore defined as:

$$K_i = \begin{cases} k_w \Delta & \text{if} \quad T_{i+1} > T_i \\ k_w & \text{if} \quad T_{i+1} \leq T_i \\ 0 & \text{if} \quad i = 0 \quad \text{or} \quad i = n \end{cases} \quad (7)$$

with k_w the water conductivity and Δ, an empirical parameter defining the strength of the convection effect. Finally, the vector $\mathbf{T}^t$ at time t can be obtained by solving n equations with n unknowns, knowing the temperature distribution at the previous time step $\mathbf{T}^{t-1}$ and that can be rewritten in matrix form and solved using an explicit integration scheme:

$$A(K, \tau, \dot{m}_u) \cdot \mathbf{T}^t + B(\tau) \cdot \mathbf{T}^{t-1} + C(k_{HR}) = 0 \quad (8)$$

with $A(K, \tau, \dot{m}_u)$, $B(\tau)$, $C(k_{HR})$ defined as:

$$A(K, \tau, \dot{m}_u) = \begin{bmatrix} \beta_1(K, \tau, \dot{m}_u) & \gamma_1(\dot{m}_u) & 0 & \cdots & & \\ \alpha_2(K) & \beta_2(K, \tau, \dot{m}_u) & \gamma_2(\dot{m}_u) & 0 & \cdots & \\ 0 & \alpha_3(K) & \beta_3(K, \tau, \dot{m}_u) & \gamma_3(\dot{m}_u) & 0 & \cdots \\ \vdots & & \ddots & \ddots & \ddots & \\ 0 & \cdots & 0 & \alpha_{n-1}(K) & \beta_{n-1}(K, \tau, \dot{m}_u) & \gamma_{n-1}(\dot{m}_u) \\ 0 & \cdots & & 0 & \alpha_n(K) & \beta_n(K, \tau, \dot{m}_u) \end{bmatrix}$$

https://doi.org/10.52202/077185-0015

$$B(\tau) = \begin{bmatrix} -\frac{m_0 c_p}{\tau} & 0 & \cdots & & \\ 0 & -\frac{m_1 c_p}{\tau} & 0 & \cdots & \\ \vdots & & \ddots & & \\ 0 & \cdots & & -\frac{m_{n-1} c_p}{\tau} & 0 \\ 0 & \cdots & & & -\frac{m_n c_p}{\tau} \end{bmatrix}$$

$$C(k_{HR}) = \begin{bmatrix} -h_{amb} A_{amb,1} T_{amb} - k_{HR} \dot{Q}_{HR,1} - F_{su,1} \dot{m}_u c_p T_{w,su} \\ -h_{amb} A_{amb,2} T_{amb} - k_{HR} \dot{Q}_{HR,2} - F_{su,2} \dot{m}_u c_p T_{w,su} \\ \vdots \\ -h_{amb} A_{amb,n} T_{amb} - k_{HR} \dot{Q}_{HR,n} - F_{su,n} \dot{m}_u c_p T_{w,su} \end{bmatrix}$$

with the terms in $A(K, \tau, \dot{m}_u)$ given by:

$$\begin{cases} \alpha_i(K) = -\frac{K_{i-1} A_c}{\mathrm{d}x} \\ \beta_i(K, \tau, \dot{m}_u) = \frac{m_i c_p}{\tau} + F_{out,i} \dot{m}_u c_p + \frac{K_i A_c}{\mathrm{d}x} + \frac{K_{i-1} A_c}{\mathrm{d}x} + h_{amb} A_{amb,i} \\ \gamma_i(\dot{m}_u) = -F_{in,i} \dot{m}_u c_p - \frac{K_i A_c}{\mathrm{d}x} \end{cases}$$

Finally, the total energy consumption/ambient heat rejection can be computed by adding the individual power consumptions/rejections multiplied by the time step. For the total energy consumption, the equation can be written as:

$$E_{elec} = \sum \dot{Q}^t_{HR,i} \cdot \tau \tag{9}$$

2.3 Influence of the time step

The selection of the time step is of paramount importance to optimize the computational efficiency of the model. A low time step will tend to give high accuracy with high computational time and conversely. When finding the optimal time step, it is important to define the two working phases of the water heater:

- The charging phase: corresponds to the period when no water is used, the water is heated up until a set point is reached, afterwards, the water heater is at rest, only losing some heat trough ambient heat transfer. The water heater tends to be most the time in this phase and quick dynamics are not involved. As can be seen in **Figure** 5, a time step of 180 s can be used without affecting the model accuracy. However, the control does not allow to stop the heating system during the 3 last minutes of heating, resulting in a slightly higher temperature in the bottom nodes. It is important to note that 100 nodes have been selected not to induce a bad accuracy due to a too low number of nodes. A time step of 60 s has finally been chosen.
- The discharging phase: is usually a quick phase, especially when the storage volume is low. High dynamics are involved in this phase and a low time step is therefore necessary, as can be seen in **Figure** 6. A time step of 2 s has finally been chosen.

2.4 Influence of the number of nodes and simulation time

The selection of the ideal number of nodes results in a trade-off between accuracy and computation time. For example, using a high number of nodes will theoretically be more accurate but is more computationally intensive. Furthermore the simulation time is strongly related to the number of nodes used to model the water storage tank. On the one hand, the resolution process (**Equation** 6) is dependent on the matrices size and will obviously take more time when large matrices are used. On the other hand, the construction of these matrices themselves is computationally consuming. Therefore, the computation

https://doi.org/10.52202/077185-0015

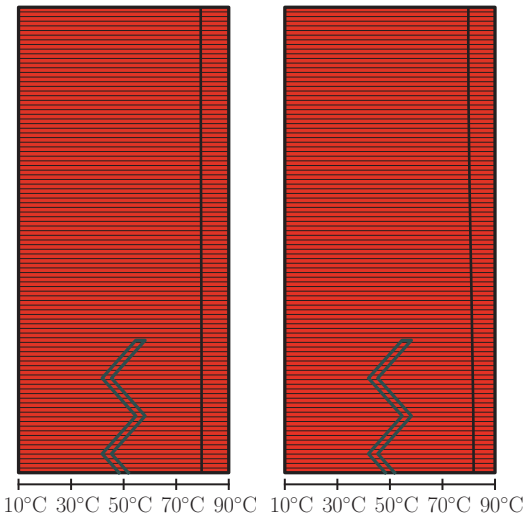

(a) $\tau = 1$ s **(b)** $\tau = 180$ s

Figure 5: Temperature profile after 2h of charge from a uniform temperature of 20°C for different time steps.

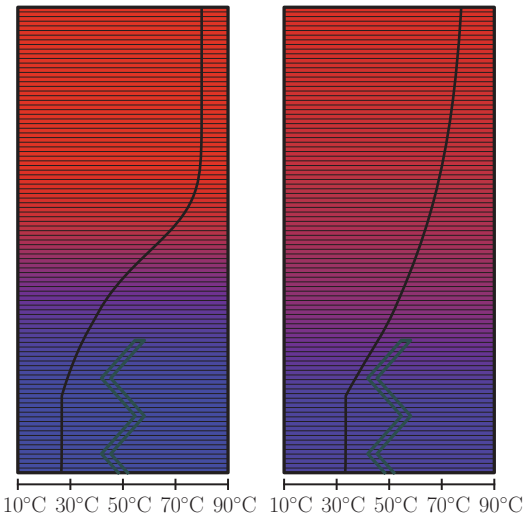

(a) $\tau = 1$ s **(b)** $\tau = 120$ s

Figure 6: Temperature profile after 4 minutes of discharge from a uniform temperature of 80°C for different time steps.

time can be divided in three parts:

- The initialization time, slightly varying with the number of nodes
- The matrices construction time, varying linearly with the number of nodes as the number of non-zero terms is proportional to the size of the matrices
- The system resolution time, varying cubically with the number of nodes as numpy perfom a LU decomposition to inverse a matrix

The present model proposes an optimization of the computation time, optimizing the matrices definition process. The matrices definition is actually not needed for each time iteration, as under some conditions, the matrices remain the same from one time iteration to the following. A new matrix definition is necessary when a temperature inversion phenomenon is met (i.e., the temperature of a top layer is lower than the temperature of a bottom layer), typically occuring when heating, resulting in a change of the conduction/convection coefficient defined in **Equation** 7. It is also necessary to redefine the matrices when the water heater stops heating and stays at rest (coefficient k_{HR} changing in **Equation** 6). Finally, a redefinition of the matrices is also needed when the mass flow rate changes. In each iteration where none of the conditions mentioned are met, no recalculation of the matrices is done, which can significantly reduce the simulation time. The problem can be formulated in mathematical form as:

$$\begin{aligned}
&\texttt{if } \dot{m}_{su}^{t} \neq \dot{m}_{su}^{t-1} \texttt{ or } k_{HR}^{t} \neq k_{HR}^{t-1} \texttt{ or } T_{k-1}^{t-1} > T_{k}^{t-1}\ \forall k \in [0,n]: \\
&\quad A^{t} = A(K^{t}, \tau, \dot{m}_{u}^{t});\ B^{t} = B(\tau);\ C^{t} = C(k_{HR}^{t}) \quad \text{Recompute the matrices} \\
&\texttt{else}: \\
&\quad A^{t} = A^{t-1};\ B^{t} = B^{t-1};\ C^{t} = C^{t-1} \quad \text{Keep the same matrices}
\end{aligned}$$

In **Figure** 7, a comparison between the model resolution time and results with and without optimization is made. The simulations are based on the water usage scenario defined in **Figure** 10 over one week. To select the right number of nodes, the final electricity consumption over the week is also displayed. As can be seen, the latter stabilizes at around 40 nodes, which seems to be an ideal number providing good accuracy without increasing significantly the computation time. The total computation time for a number

https://doi.org/10.52202/077185-0015

of nodes of 40, making use of the optimization process, is 17.5 s, resulting in a real time to computational time ratio of 35000. The optimization process allows computation time relative reductions of 60% for 10 nodes, 45% for 40 nodes and 36% for 100 nodes.

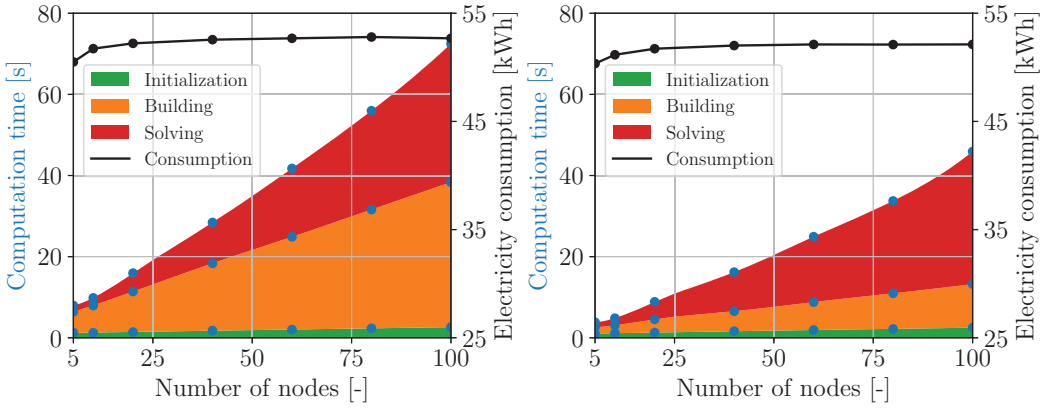

(a) Without optimization.

(b) With optimization.

Figure 7: Computation time and resulting electricity consumption varying with the number of nodes of each tank, with and without optimization process.

3 MODEL VALIDATION

The objective of the model is to provide the electrical power consumption as well as the temperature of the water available at the outlet as a function of time. The inputs of the model are the water mass flow rate consumption over time as well as the ambient and the water supply temperature over time. The parameters include the storage tank dimensions, the characteristics of the heating system and three empirical parameters that must be fitted according to experimental data. In this section, the three empirical parameters fitting is detailed, and the validation of the model outputs with regards to experimental data will be shown. Regarding the validation of the model, three types of validation are carried out:

- Variation of the water storage total energy when at rest. Allows to figure out the ambient heat losses and to define its semi-empirical parameters h_{amb}.
- Variation of the electrical consumption over time under a water usage scenario. Allows to validate the condution/convection empirical parameter Δ.
- Variation of the stratification during a discharge phase under constant mass flow rate: allows to validate the water injection height (empirical parameter H_{mix}).

The second point requires the perfect knowledge of the default control strategy of the selected water heater. This control strategy will therefore be experimentally tested in order to implement it in the model. The (semi-) empirical parameters set after the mentioned investigations can be found in **Table** 1. They have been found manually by minimizing the Mean Absolute Error (MAE) for the heat loss and temperature stratification tests (allowing to get respectively h_{amb} and H_{mix}), and by minimizing the total energy consumption in the power consumption test allowing to estimate Δ.

3.1 Experimental setup

The validation of the model requires experimental data. To this aim, a test bench has been built, enabling to investigate experimentally the EWH (Ariston Velis Evo Dry Flexible Wifi) in a climate chamber. An electronically controlled valve along with a manual needle valve allow to simulate the water flow rate demand. The inlet and outlet temperatures of the water are measured with thermocouples introduced

https://doi.org/10.52202/077185-0015

Table 1: Empirical parameter values of the calibrated model.

Parameter	Value
h_{amb}	0.8 [W/(m^{2}K)]
Δ	10000 [-]
H_{mix}	0.15 [m]

in sleeves and the mass flow rate is figured out with a water meter connected to a frequency meter. The temperature stratification is investigated using thermocouples placed on the tank surfaces, under the insulation layer. It allows to get the water temperature with a good accuracy without introduction of temperature sensors inside the tanks, although some dynamic effects create a time delay between the water and the tank surface temperatures. The thermocouples on the tank surfaces are distributed every 10 cm over the tanks height. The electrical power consumption of each tank is investigated using power meters placed in series with their electrical supply.

3.2 Control strategy

Given the lack of indication regarding the EWH temperature control strategy, the latter had to be studied experimentally. To that aim, the EWH temperature set point has been fixed at 80°C for more than 24h, without any water usage. The temperature feedback of the controller (placed inside a tube at approximately 30 cm from the bottom) is reported in **Figure** 8, along with the electrical power consumption of each tank resistor.

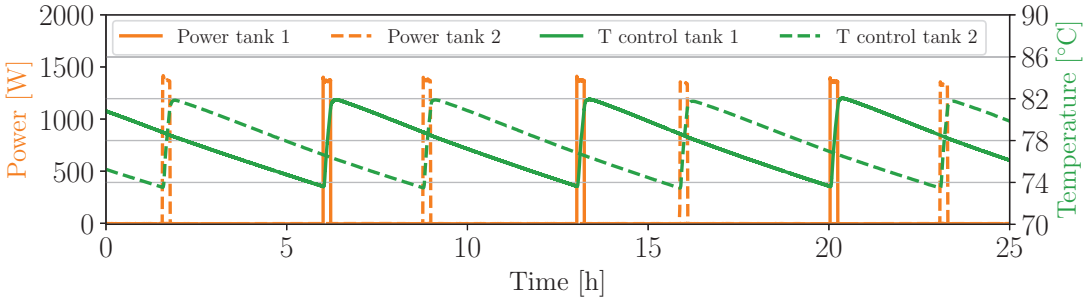

Figure 8: Evolution of control temperatures and resistor powers in each tank.

As can be understood in **Figure** 8, the temperature set point is exceeded by 2 K and the control temperature goes 6 K below the setpoint before restarting the heating resistor, avoiding the intensive use of mechanical relays to one switch every ~ 7 hours. It has also been noticed that the two heating resistors never work at the same time, and the priority is always given to the tank number two, providing the user with hot water.

3.3 Variation of the heat losses and electrical power consumption

The validation of the heat loss model allows to calibrate the ambient heat transfer coefficient (semi-empirical parameter h_{amb}). To that end, the water heater has been heated up to a 80°C set point resulting in a starting average temperature of 75.5°C in the EWH. Then, the EWH average temperature decrease has been recorded for 70 hours (heater off) as can be seen in **Figure** 9. The average ambient temperature recorded is 18°C. At the beginning of the experiment (at ~ 75°C), the ambient heat loss is equal to 70 W, while at ~ 40°C, it is equal to 22 W. The resulting calibrated semi-empirical parameter is h_{amb} = 0.8 W/(m^{2}K).

To investigate the electrical power consumption, a water usage profile has been simulated and experimentally tested. This scenario comprises a heat up from a uniform 15°C temperature profile in both tanks (set point of 80°C). Then two 10-minute showers have been emulated, with a water mass flow rate of 80

https://doi.org/10.52202/077185-0015

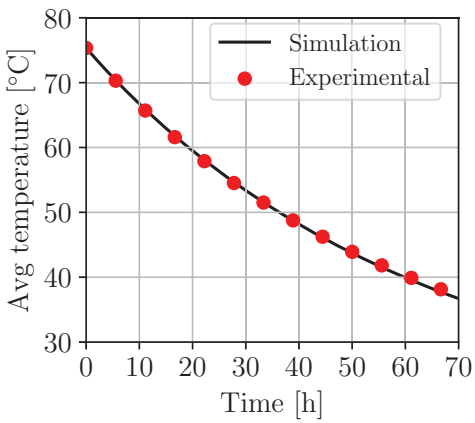

Figure 9: Evolution of the average water temperature in the tanks as a function of time.

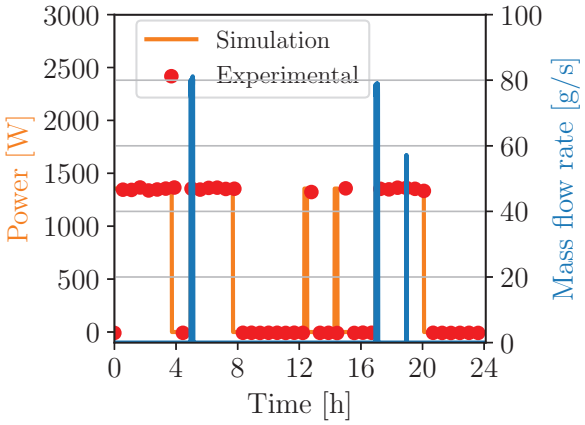

Figure 10: Evolution of the power consumption of the water heater over 24 h under a water usage scenario.

g/s (10 L/min at 38°C), 12 hours apart. Finally, a 2-minute dish wash of 55 g/s has been added 2 hours later. This 24-hour scenario has been tested/emulated and the results from the experimental campaign and the simulation compared, as can be seen in **Figure** 10. As can be observed, the model predicts quite well the real behavior of the EWH, with a total electricity consumption of 13.6 kWh against 14 kWh experimentally recorded (~ 3% of relative error). It is important to note that the empirical parameter Δ has been set at 10000 (a higher value could also work), as the temperature profile behaves like a vertical lign when heating up (similar to a direct heat transfer from the bottom to the top).

3.4 Variation of the temperature stratification profile

The investigation of the temperature stratification has been carried out using a constant mass flow rate of 80 g/s during 8 minutes, from a fully charged EWH (set point of 80°C). The semi-empirical mixing height (H_{mix}) has been set to 15 cm, allowing to mix the inlet cold water with the hot water in the bottom nodes (on a 15-cm height). If this parameter was set to zero, the bottom of the tank would be at the supply water temperature (15°C), which is not the case experimentally. Two temperature stratification profiles can be found in **Figure** 11. The left figure shows the profile after 3 minutes of discharge, a temperature difference is noticeable at the temperature changing zone (transition between hot and cold water), this can be explained by the time delay introduced by the temperature measured at the surface of the metallic tanks, and not inside it. The right figure shows the profile after 8 minutes of discharge + 3 hours of stabilization, the simulated temperature profile fits well with the experimental points recorded with 1.6 K of MAE.

4 CONCLUSION

In this paper, a model of electrical water heater, intended to be used for demand response enhancement, has been presented. The multi-node approach seemed to be the most convenient and effective way to model an electrical water heater, combining good accuracy and low computational time. The effects of both time step and nodes number have been investigated, and an optimization of the computation time proposed.

The model has been validated using a water heater with a specific geometry: it uses two low-diameter storage tanks to enhance temperature stratification effects. First, the heat loss through a long period of time has been validated. Then, the electricity consumption profile validated against a given water usage scenario. The matching between the simulation and experiment results have shown a good accuracy, with less than 3% of error for the total electricity consumption over 24 hours, following the proper con-

https://doi.org/10.52202/077185-0015

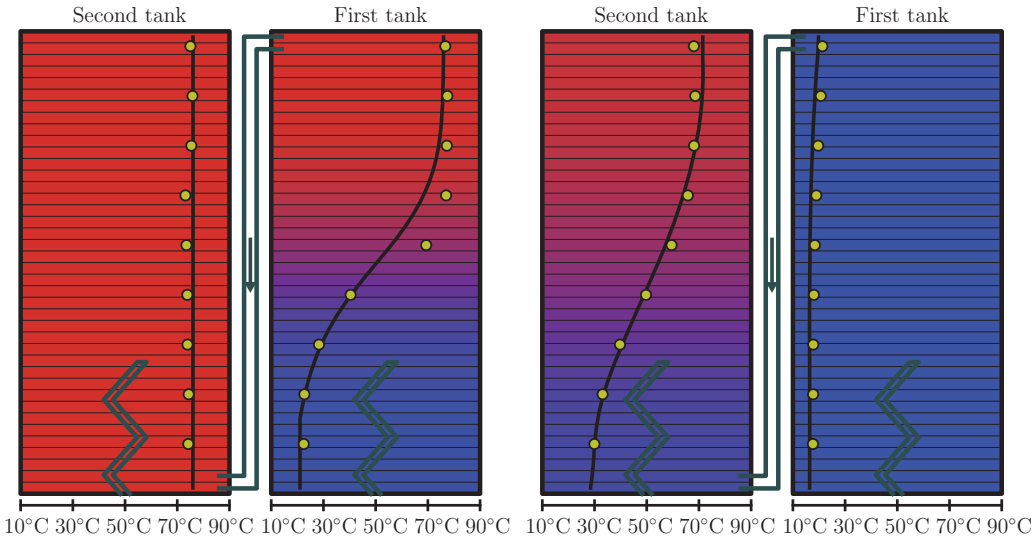

(a) After 3 minutes of discharge (MAE = 2.6 K)

(b) After 3 hours following 8 minutes of discharge (MAE = 1.6 K)

Figure 11: Temperature profile validation after a discharge of 80 g/s.

trol strategy. Finally, the temperature stratification profile has also been validated, with 1.6 K of mean absolute error along the height of both tanks. For the sake of transparency and reproducibility, which are important aspects of experimental research, the data and the source code of the model are provided under open licenses in the following repository: GitHub Link. They can bee freely downloaded, re-used and adapted.

NOMENCLATURE

EWH	electrical water heater, (−)	k_w	water heat conductivity, ((W/(mK)
n	number of nodes, (−)	c_p	specific heat capacity, (J/(kgK))
h	heat transfer coefficient, (W/(m^{2}K))	m	mass, (kg)
$\dot{m}$	mass flow rate, (kg/s)	τ	time step, (s)
H	height, (m)	A	surface, (m^2)
$\dot{Q}$	heat transfer rate, (W)	K	heat tranfer coefficient, (W/(mK))
Δ	empirical parameter, (−)	τ	time step, (s)
k	parameter, (J/kgK)		

Subscripts and superscripts

HR	heating resistor	out	outlet
SP	set point	su	supply
u	usable	amb	ambient
sto	storage	max	maximum
w	water	mix	mixing
$elec$	electric	l	layer
in	inlet	c	circular

https://doi.org/10.52202/077185-0015

REFERENCES

IEA, Belgium - Countries and Regions. `https://www.iea.org/countries/belgium`. Accessed: 2024-01-22.

Beeker, N., Malisani, P., and Petit, N. (2015). Dynamical modeling for electric hot water tanks. volume 48, pages 78–85. Elsevier B.V.

Deutz, K. R., Cauret, O., Rullière, R., and Haberschill, P. (2016). Modeling and experimental study of a heat pump water heater cycle. International Refrigeration and Air Conditioning Conference proceedings.

Diao, R., Lu, S., Elizondo, M., Mayhorn, E., Zhang, Y., and Samaan, N. (2012). Electric water heater modeling and control strategies for demand response.

Dickes, R., Desideri, A., Lemort, V., and Quoilin, S. (2015). Model reduction for simulating the dynamic behavior of parabolic troughs and a thermocline energy storage in a micro-solar power unit. ECOS conference proceedings.

Duffie, J. A. and Beckman, W. A. (2013). *Solar engineering of thermal processes*. Wiley.

Dumont, O., Carmo, C., Georges, E., Dickes, R., Quoilin, S., and Lemort, V. (2016). Hot water tanks : How to select the optimal modelling approach?

Missaoui, S., Driss, Z., Slama, R. B., and Chaouachi, B. (2023). *Numerical and Experimental Study of the Heat Pump Water Heater with an Immersed Helical Coil Heat Exchanger*. IntechOpen.

Nash, A. L., Badithela, A., and Jain, N. (2017). Dynamic modeling of a sensible thermal energy storage tank with an immersed coil heat exchanger under three operation modes. *Applied Energy*, 195:877–889.

Paolesi, R. and Stopponi, A. (2011). Flat water heater with reduced capacity storage tanks.

Powell, K. M. and Edgar, T. F. (2013). An adaptive-grid model for dynamic simulation of thermocline thermal energy storage systems. *Energy Conversion and Management*, 76:865–873.

Quynh, N. M., Lepivert, X., and Guerassimoff, G. (2022). Methodology of building a water heater aggregated model for evaluating energy flexibility for domestic hot water.

Salameh, W., Faraj, J., Harika, E., Murr, R., and Khaled, M. (2021). On the optimization of electrical water heaters: Modelling simulations and experimentation. *Energies*, 14.

Xu, Z., Diao, R., Lu, S., Lian, J., and Zhang, Y. (2014). Modeling of electric water heaters for demand response: A baseline pde model. *IEEE Transactions on Smart Grid*, 5:2203–2210.

AKNOWLEDGEMENT

The project source of the results presented in this paper has received funding from the Belgian Energy Transition Fund (Belgian Energy Transition Fund).

https://doi.org/10.52202/077185-0015